Quantitative Susceptibility Map Reconstruction via a Total Generalized Variation regularization

Felipe Yanez*†, Audrey Fan‡, Berkin Bilgic‡, Carlos Milovic*†, Elfar Adalsteinsson‡§ and Pablo Irarrazaval*†
*Department of Electrical Engineering,
Pontificia Universidad Católica de Chile,
Santiago, Chile
†Biomedical Imaging Centre,
Pontificia Universidad Católica de Chile,
Santiago, Chile
‡Department of Electrical Engineering and Computer Science,
Massachusetts Institute of Technology,
Cambridge, MA, United States
§Harvard-MIT Division of Health Sciences and Technology,
Cambridge, MA, United States

***Abstract*—Quantitative susceptibility mapping (QSM) is a last decade new concept which allows to determine the magnetic susceptibility distribution of tissue in-vivo. Nowadays it has several applications such as venous blood oxygenation and iron concentration quantification. To reconstruct high quality maps, a regularized scheme must be used to solve this ill-posed problem, due to the dipole kernel undersampling k-space. A widely used regularization penalty is Total Variation (TV), however, we can find staircasing artifacts in reconstructions due to the assumption that images are piecewise constant, not always true in MRI. In this sense, we propose a less restrictive functional, to avoid this problem and to improve QSM quality. A second order Total Generalized Variation (TGV) does not assume piecewise constancy in the images and is equivalent to TV in terms of edge preservation and noise removal. This work describes how TGV penalty addresses an increase in imaging efficiency in magnetic susceptibility maps from numerical phantom and in-vivo data. Currently, we report higher specificity with the proposed regularization. Moreover, the robustness of TGV suggest that is a possible alternative to tissue susceptibility mapping.**

***Keywords*-Quantitative susceptibility mapping; Brain; Total Generalized Variation**

I. Introduction

Previous work has shown that Quantitative Susceptibility Mapping (QSM) is a relatively new concept which allows determining the magnetic susceptibility distribution of tissue in-vivo [1]. Nowadays, QSM has several applications, such as venous blood oxygenation [2] and iron concentration quantification [3].

To reconstruct high quality maps, a regularized scheme must be used to solve this ill-posed problem, since the dipole kernel undersamples k-space. Therefore, to promote sparsity in the penalty, the emergence of l_1 norms such as Total Variation (TV) have been a valuable and widely used scheme [2], [4]. However, this regularization may lead to staircasing artifacts [5] in the presence of B_1 inhomogeneity becauseTV assumes images are piecewise constant, not always true in MRI.

To avoid this problem and to improve QSM quality we propose a less restrictive functional: a second order Total Generalized Variation (TGV). This penalty does not assume piecewise constant images (free of staircasing artifacts) and is equivalent to TV in terms of edge preservation and noise removal [5]. We report high quality QSM from numerical phantom and in-vivo data using a TGV optimization algorithm, similar to the one used in compressed sensing [6].

II. Theory

In general, it is known that B, the measured normalized field map in k-space, is defined as the convolution between the susceptibility kernel d and the susceptibility distribution χ [7], [8]. Now, to quantify tissue magnetic susceptibility, χ maps, the following system of linear equations must be solved:

$$B = d * \chi \tag{1}$$

For simplicity, the spatial convolution in Equation (1) could be expressed in the Fourier domain as follows:

$$b = F^{-1} D F \chi \tag{2}$$

where b is the normalized field map, F is the Fourier transform operator, $D = 1/3 - {k_z}^2/(k_x^2 + k_y^2 + k_z^2)$ is the susceptibility kernel in k-space and χ is the susceptibility

978-0-7695-5061-9/13 $26.00 © 2013 IEEE
DOI 10.1109/PRNI.2013.59

distribution [9].

An important issue for susceptibility distribution reconstruction is that the dipole kernel in k-space severally undersamples the measured field [3], [8]. This happens at the magic angle of $54,6^o$ along a conical surface in k-space. Therefore Equation (2) is an ill-posed problem. To find a high quality estimation of χ for this problem, we require to solve the regularized version of Equation (2). It is also known that the gradient of underlying susceptibility distribution is sparse, therefore, an appropriate sparse transformation will help to solve the problem [3], [4]. In several QSM applications, reconstructions of χ maps are done via l_1 frameworks, setting a Total Variation penalization [4], [3], [10].

In contrast to the previous approach, we propose a second order Total Generalised Variation (TGV) penalty. TGV is the semi-norm of a Banach space, where associated variational problems fit well into the well-developed mathematical theory of convex optimization problems. Moreover, each function of bounded variation admits a finite TGV value, meaning in particular that piecewise constant images can be captured with TGV which even extends TV [5]. In other words, TGV does not assume that the images consist of regions and is equivalent to TV in terms of edge preservation and noise removal.

In this work, we propose to address the reconstruction of χ map by solving the regularized version of Equation (2), considering the noise level in the λ regularization parameter:

$$\hat{\chi} = \min_{\chi \in L^2(\Omega)} TGV(\chi) + \lambda ||b - F^{-1} D F \chi||_{l_2}^2 \qquad (3)$$

where,

$$TGV(\chi) = \arg\min_{\psi \in \Omega} \int_\Omega |\nabla\chi - \psi| dx + \beta_0 \int_\Omega |\nabla\psi - \nabla\psi^T| dx \qquad (4)$$

considering ψ as an auxiliary vector field in the gradient domain.

III. Methods

To test the proposed regularization, we reconstruct the susceptibility χ map from numerical phantom and noisy in-vivo field maps using TV and TGV algorithms, and compare performances. We use a similar optimization algorithm to that used in compressed sensing [6].

For the numerical phantom (120×120×78) we computed a piecewise non-constant susceptibility map. We defined three regions: gray matter ($\chi = 0.027$ ppm), cerebrospinal fluid ($\chi = -0.018$ ppm) and white matter ($\chi = -0.023$ ppm). To avoid non-constant regions we added noise to each region with a variance of 10% of the original value.

In-vivo data was acquired from a healthy volunteer using a 3D Spoiled Gradient Recalled Echo (SPGR) sequence at 1.5T. 62 axial slices with 2.5 mm slice thickness and FOV of 240×240×155 mm^3 with a $TR/TE = 58ms/40ms$ and 512×256 resolution in-plane [10].

An important issue in TGV is setting the weights λ and β_0. For β_0-tuning we perform a general cross validation [11] over the TGV functional in Equation (4). After validation, our model learned an optimum regularization parameter of $\beta_0 = 1.86$, which compares reasonably with the literature [5]. Finally, λ is set by using the L-curve method between the penalty and data consistency [10]. Optimal settings for TV and TGV penalties are $\lambda = 2 \cdot 10^{-2}$ and $\lambda = 8 \cdot 10^{-5}$ respectively.

IV. Results

Herein are presented the results of the susceptibility reconstructions from numerical phantom and noisy in-vivo field map using TV and TGV algorithms.

A. Numerical phantom

For numerical susceptibility reconstruction we ran both algorithms, results in Figure 1, where we can clearly appreciate tissues that are recovered by TGV and not by TV. In the pointed out ROI of Figure 1, we can appreciate that TGV has better performance in non-constant regions. We can report: χ_{TRUE} = 0.025 ppm, χ_{TV} = 0.019 ppm and χ_{TGV} = 0.022 ppm in the ROI of Figure 1.

In Figure 2 we present χ values through a sagittal profile, as defined in Figure 1 (*center*); TGV is closer to true data in non-constant regions than TV, where we report a root-mean-square error (RMSE) of 4.8% for TV and 2.9% for TGV. In constant regions they perform almost the same, having only numerical error, RMSE of 0.2%.

B. In-vivo data

For in-vivo reconstruction we used a field map with 200 iterations of dipole fitting. In Figure 3 we present reconstructions using both penalties. We can appreciate that TGV and TV reconstructions look alike, but it is clear the quality of structure definition while comparing. The TGV penalty could recover and define structures that the TV penalty could not. In Figure 4 we show a ROI of previous reconstructions, where we can appreciate two effects: staircasing artifacts and structure definition (better

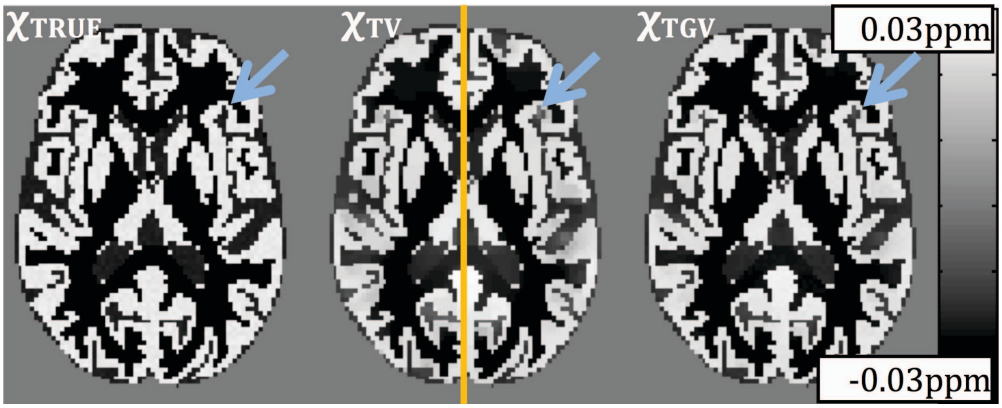

Figure 1. True axial χ view (*left*), reconstruction using TV penalty (*centre*) and reconstruction using TGV penalty (*right*).

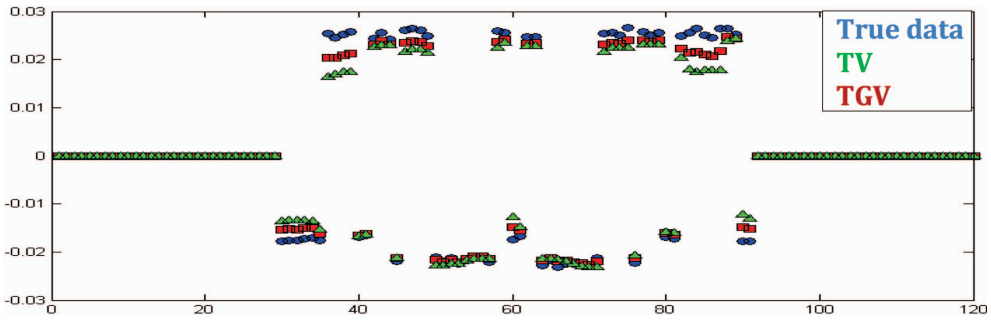

Figure 2. Intensity of χ map (in ppm) through a sagittal profile (see Figure 1).

resolution). We also verify that staircasing artifacts in the vessel are smoothed and the structure is clearly defined via TGV. Finally, in Figure 5 we present the absolute difference map between the two penalties in an axial in-vivo χ map reconstruction, where we can appreciate the structures that differed in both methods.

C. Computational cost

To run the algorithms, we used a processor Intel(R) Core(TM) i7-2600 CPU @ 3.40 GHz and Installed memory (RAM) of 16.0 GB. We report that TV convergence is in 1,629.0 seconds with 100 conjugate gradient iterations, and convergence via TGV regularization is in 1,551.0 seconds with 80 conjugate gradient iterations.

V. Conclusion

Two regularized QSM algorithms are presented, employing TV and TGV penalties, which successfully remove background phase effects via dipole fitting and solve for the tissue susceptibility distribution via convex optimization. The performance in image efficiency, structure definition and computational cost of TGV was favorable over TV on numerical phantom and in-vivo data.

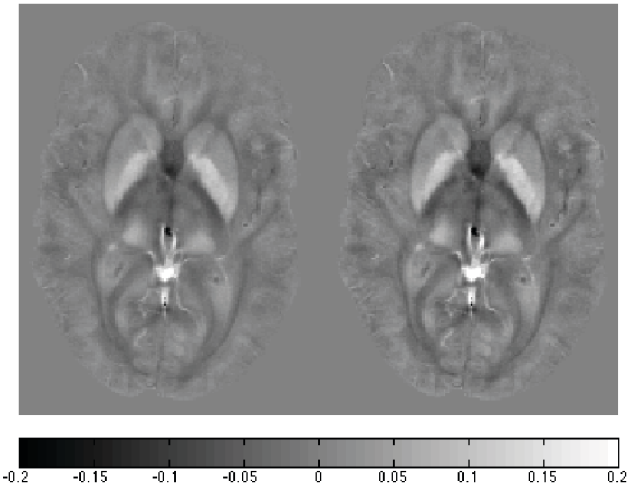

Figure 3. Axial in-vivo χ map reconstruction (in ppm) using TV (left) and TGV (right) with optimum settings.

Acknowledgment

The author Felipe Yanez acknowledges financial support from MIT's MISTI-UC Program and appreciates all the help offered by the MRI Group at MIT.

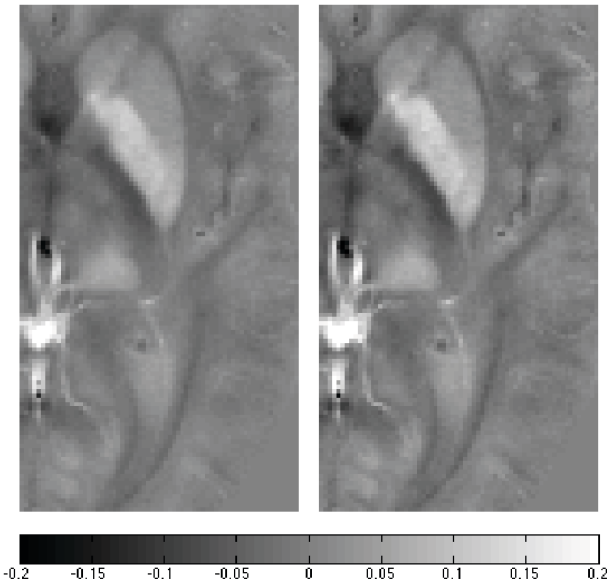

Figure 4. Vessel ROI of in-vivo χ map (in ppm) for TV (left) and TGV (right) optimum-setting-reconstructions.

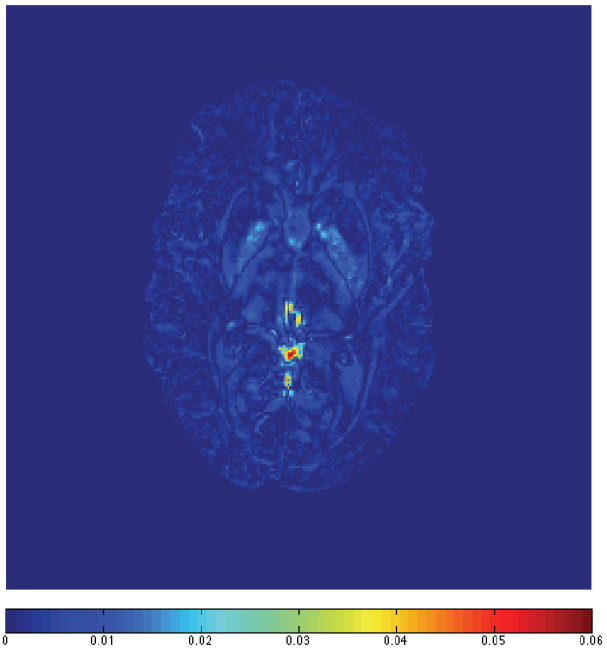

Figure 5. Absolute difference map (in ppm) between TV and TGV axial in-vivo χ map reconstructions.

REFERENCES

[1] C. Langkammer, F. Schweser, N. Krebs, A. Deistung, W. Goessler, E. Scheurer, K. Sommer, G. Reishofer, K. Yen, F. Fazekas, S. Ropele, and J.R. Reichenbach, "Quantitative susceptibility mapping (QSM) as a means to measure brain iron? A post mortem validation study," *Neuroimage*, 62(3):1593-1599, 2012.

[2] A. P. Fan, T. Benner, D. S. Bolar, B. R. Rosen, and E. Adalsteinsson, "Phase-based Regional Oxygen Metabolism (PROM) at 3T and feasibility at 7T," in *Proceedings of the 18th Annual Meeting of International Society for Magnetic Resonance in Medicine*, Stockholm, Sweden, 2010, pp. 693.

[3] J. Liu, T. Liu, L. de Rochefort, I. Khalidov, M. Prince, and Y. Wang, "Quantitative susceptibility mapping by regulating the field to source inverse problem with a sparse prior derived from the Maxwell Equation: validation and application to brain," in *Proceedings of the 18th Annual Meeting of International Society for Magnetic Resonance in Medicine*, Stockholm, Sweden, 2010, pp. 4996.

[4] A. P. Fan, B. Bilgic, T. Benner, B. R. Rosen, and E. Adalsteinsson, "Regularized Quantitative Susceptibility Mapping for Phase-based Regional Oxygen Metabolism (PROM) at 7T," in *Proceedings of the 19th Annual Meeting of International Society for Magnetic Resonance in Medicine*, Montreal, Canada, 2011, pp. 4472.

[5] F. Knoll, K. Bredies, T. Pock, and R. Stollberger, "Second order total generalized variation (TGV) for MRI," *Magnetic Resonance in Medicine*, 65(2):480-491, 2011.

[6] M. Lustig, D. L. Donoho, and J. M. Pauly, "Sparse MRI: The Application of Compressed Sensing for Rapid MR Imaging," *Magnetic Resonance in Medicine*, 58(6):1182-1195, 2007.

[7] R. Salomir, B. De Senneville, and C. Moonen, "A fast calculation method for magnetic field inhomogeneity due to an arbitrary distribution of bulk susceptibility," *Concepts in Magnetic Resonance*, 19B: 2634, 2003.

[8] J. P. Marques, and R. Bowtell, "Application of a Fourier-based method for rapid calculation of field inhomogeneity due to spatial variation of magnetic susceptibility," *Concepts in Magnetic Resonance Part B: Magnetic Resonance Engineering*, 25B: 65-78, 2005.

[9] B. Bilgic, A. P. Fan, and E. Adalsteinsson, "Quantitative Susceptibility Map Reconstruction with Magnitude Prior," in *Proceedings of the 19th Annual Meeting of International Society for Magnetic Resonance in Medicine*, Montreal, Canada, 2011, pp. 746.

[10] B. Bilgic, A. Pfefferbaum, T. Rohlfing, E. V. Sullivan, and E. Adalsteinsson, "MRI estimates of brain iron concentration in normal aging using quantitative susceptibility mapping," *Neuroimage*, 59(3): 2625-2635, 2012.

[11] S. Arlot, and A. Celisse. "A survey of cross-validation procedures for model selection," *Statistics Surveys*, vol. 4, pp. 40-79, 2010.